

# Capacity and outage analysis of a dual-hop decode-and-forward relay-aided NOMA scheme

Md. Fazlul Kader, Mohammed Belal Uddin, and Soo Young Shin

**Abstract**—Non-orthogonal multiple access (NOMA) is regarded as a candidate radio access technique for the next generation wireless networks because of its manifold spectral gains. A two-phase cooperative relaying strategy (CRS) is proposed in this paper by exploiting the concept of both downlink and uplink NOMA (termed as DU-CNOMA). In the proposed protocol, a transmitter considered as a source transmits a NOMA composite signal consisting of two symbols to the destination and relay during the first phase, following the principle of downlink NOMA. In the second phase, the relay forwards the symbol decoded by successive interference cancellation to the destination, whereas the source transmits a new symbol to the destination in parallel with the relay, following the principle of uplink NOMA. The ergodic sum capacity, outage probability, and outage sum capacity are investigated comprehensively along with analytical derivations, under both perfect and imperfect successive interference cancellation. The performance improvement of the proposed DU-CNOMA over the conventional CRS using NOMA, is proved through analysis and computer simulation. Furthermore, the correctness of the author's analysis is proved through a strong agreement between simulation and analytical results.

**Index Terms**—Cooperative relaying, Downlink, Ergodic capacity, Non-orthogonal multiple access, Successive interference cancellation, Uplink.

## I. INTRODUCTION

To deal with the high data rate requirements of the next generation wireless networks, integration of multiple technologies is anticipated [1, 2]. Cooperative relaying strategy (CRS) is an important technology for wireless networks to improve system capacity, combat fading, and extend service coverage [3]. In addition, non-orthogonal multiple access (NOMA) has garnered substantial attention from the industry and academia, to meet with the large data rate requirements of 5G and beyond [4-6]. In this paper, cooperative diversity and NOMA is integrated, which can be a promising approach to meet the capacity demands for future wireless networks [7-9].

A lot of different varieties of NOMA can be found in the literature [10]. Among them, cooperative NOMA (C-NOMA) is one of the most dynamic areas of research [7-12]. Based on the direction of data transmission C-NOMA can be further classified as uplink C-NOMA [13-14] and downlink C-NOMA [15-17]. In [15], a cooperative relaying scheme (CRS) using NOMA (termed as CRS-NOMA) was proposed to improve the spectral efficiency over independent Rayleigh fading channels, where a source (S) transmits a superposition coded composite signal to the relay (R) and the destination (D), during the first time slot. Then, R decodes own symbol by

performing successive interference cancellation (SIC), whereas D decodes own symbol considering other signal as noise. In the subsequent time slot, R retransmits the decoded symbol with full power to D. In [16], the performance of CRS-NOMA [15] was investigated over Rician fading channels. A novel detection scheme for CRS-NOMA [15] was proposed in [17] (termed as CRS-NOMA-ND), where D uses maximal-ratio combining and another SIC to jointly decode transmitted symbols by source. Note that only achievable average rate was analyzed in [15-17]. In [18-19], the authors considered both uplink and downlink NOMA under non-cooperative scenario, whereas [20-21] exploited the concept of both uplink and downlink NOMA under cooperative scenario. In [20], a cooperative relay sharing network was proposed, where multiple sources can communicate with their corresponding destination simultaneously through a common relay. A C-NOMA scheme considering both downlink and uplink transmission systems, was proposed in [21], where a strong user works as a cooperative relay for the weak user.

Unlike the existing works, in this paper, a CRS-NOMA scheme using the concept of downlink and uplink NOMA (termed as DU-CNOMA) is proposed. In the proposed DU-CNOMA, S transmits a superposition coded composite signal consisting of two symbols  $s_1$  and  $s_2$  to D and R, according to the principle of downlink NOMA as in [15-17], during the first time slot. However, in the subsequent time slot, unlike [15-17], S transmits a new symbol  $s_3$  and R transmits decoded symbol  $s_2$  to D simultaneously, according to the principle of uplink NOMA [13, 18-19]. Furthermore, unlike [15-17], where only perfect SIC is considered, we consider both perfect and imperfect SIC by taking into account a more realistic scenario. Principal contributions of this paper are outlined as follows:

- 1) A dual-hop CRS by taking into account NOMA, is proposed and investigated over independent Rayleigh fading channels.
- 2) The closed-form expressions of the ergodic sum capacity (ESC), outage probability (OP), and outage sum capacity (OSC) of DU-CNOMA are derived under both perfect and imperfect SIC. The analytical results are validated by Monte Carlo simulation.
- 3) The performance improvement of the proposed DU-CNOMA over CRS-NOMA [15], and CSR-NOMA-ND [17], is manifested through analysis and simulation. Moreover, analytical derivations are validated by computer simulation.

The rest of this paper is organized as follows. The system model with detailed description of the proposed protocol is provided in Section 2. The channel model is also demonstrated in this section. The closed-form expressions of the ESC, OP, and OSC are presented in Section 3, 4, and 5, respectively. The

Manuscript received XXX, XX, 2018; revised XXX, XX, 2018.

Md. Fazlul Kader is with the Department of Electrical and Electronic Engineering, University of Chittagong, Chittagong-4331, Bangladesh (email: f.kader@cu.ac.bd). Mohammed Belal Uddin, and Soo Young Shin are with the Department of IT Convergence Engineering, Kumoh National Institute of Technology, Gumi 39177, South Korea

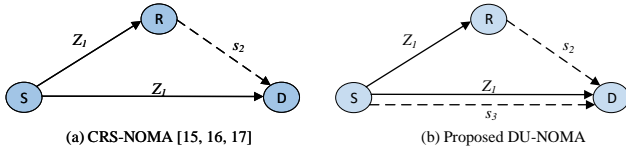


Fig. 1. System model: (a) CRS-NOMA [15-17] and (b) Proposed DU-CNOMA.

numerical results that are validated by Monte Carlo simulation, are provided in Section 6, and finally, the conclusion along with future recommendations is drawn in Section 7..

## II. NETWORK ARCHITECTURE AND PROTOCOL DESCRIPTIONS

A half-duplex cooperative relaying protocol exploiting the concept of both downlink and uplink NOMA is proposed. The system architecture consists of a source (S), a DF relay (R), and a destination (D), as drawn in Fig. 1. Fig. 1(a) shows the system architecture considered in [15-17], whereas Fig. 1(b) shows the system architecture of the proposed DU-NOMA. All the links (i.e., S-to-R, S-to-D, and R-to-D) are considered available and subjected to independent Rayleigh fading. Channel coefficient with zero mean and variance  $\lambda_i = d_i^{-\nu}$  is represented by  $h_i \sim CN(0, \lambda_i)$ , where  $d$  is the distance,  $\nu$  is the path loss exponent, and  $i \in \{1, 2, 3\}$ . Parameters  $h_1$ ,  $h_2$ , and  $h_3$  refer to the respective complex channel coefficient of S-to-D, S-to-R, and R-to-D links. Without loss of generality, it is assumed that  $\lambda_1 < \lambda_2$  and  $\lambda_1 < \lambda_3$ , under statistical channel state information [21]. The data transmission in the proposed protocol is performed by two cooperative phases as follows.

### A. Phase-1 ( $t_1$ )

At the first phase of the transmission, the source S transmits a composite NOMA signal consisting of two symbols  $Z_1 = \sqrt{\phi_1 P_s} s_1 + \sqrt{\phi_2 P_s} s_2$  to D and R simultaneously as per law of downlink NOMA. The symbols  $s_1$  and  $s_2$  are correspond to D and R, respectively. The total transmit power of S, the power allocation factor with  $s_1$ , and the power allocation factor with  $s_2$  are respectively denoted by  $P_s$ ,  $\phi_1$ , and  $\phi_2$  wherein  $\phi_1 > \phi_2$  and  $\phi_1 + \phi_2 = 1$ . Upon receiving the signal, firstly, R extracts  $s_1$  by treating  $s_2$  as noise. Then, it performs SIC to cancel out the extracted information from the received signal and thus it extracts  $s_2$ . Hence, the received signal-to-interference plus noise ratios (SINRs) at R for symbols  $s_1$  and  $s_2$  are respectively represented by

$$\gamma_{s_1 \rightarrow s_2}^1 = \frac{\phi_1 P_s |h_2|^2}{\phi_2 P_s |h_2|^2 + \sigma^2} = \frac{\phi_1 \rho |h_2|^2}{\phi_2 \rho |h_2|^2 + 1}, \quad (1)$$

$$\gamma_{s_2}^1 = \frac{\phi_2 \rho |h_2|^2}{\phi_1 \rho |\bar{h}_2|^2 + 1}, \quad (2)$$

where  $\bar{h}_2 \sim CN(0, \kappa_1 \lambda_2)$ ,  $\rho \triangleq \frac{P_s}{\sigma^2}$  is the transmit SNR of S and  $\sigma^2$  is the noise variance. The parameters  $\kappa_1$  ( $0 \leq \kappa_1 \leq 1$ ) represents the level of residual interference at R because of SIC imperfection. As a special case, the conditions of perfect

SIC and without SIC are represented by  $\kappa_1=0$  and  $\kappa_1=1$ , respectively [13, 20]. On the other hand, D decodes  $s_1$  by recking of  $s_2$  as noise. So, the received SINR regarding symbol  $x_1$  at D is obtained as

$$\gamma_{s_1}^1 = \frac{\phi_1 \rho |h_1|^2}{\phi_2 \rho |h_1|^2 + 1}, \quad (3)$$

### B. Phase-2 ( $t_2$ )

During the second phase, according to the law of uplink NOMA, R retransmits the decoded symbol  $s_2$  and S transmits a new symbol  $s_3$  to D at the same instant of time. The respective assigned powers with  $s_2$  and  $s_3$  are  $\sqrt{P_r} \vartheta_2$  and  $\sqrt{P_s} \vartheta_3$ , where  $P_r$  is the total transmit power of the relay and  $\vartheta_2 > \vartheta_3$ . As the information related to  $s_2$  is dominant over  $s_3$  at the destination, D first decodes  $s_2$  by considering  $s_3$  as noise. After then, by applying SIC procedure, it subtracts the decoded information to get  $s_3$ . So, the received SINRs concerning  $s_2$  and  $s_3$  at D are respectively given by

$$\gamma_{s_2}^2 = \frac{\vartheta_2 P_r |h_3|^2}{\vartheta_3 P_s |h_3|^2 + \sigma^2} = \frac{\vartheta_2 \rho |h_3|^2}{\vartheta_3 \rho |h_3|^2 + 1}, \quad (4)$$

$$\gamma_{s_3}^2 = \frac{\vartheta_3 \rho |h_1|^2}{\vartheta_2 \rho |\bar{h}_3|^2 + 1}, \quad (5)$$

where  $\bar{h}_3 \sim CN(0, \kappa_2 \lambda_3)$ ,  $\rho \triangleq \frac{P_r}{\sigma^2}$  is the transmit SNR by R, and  $\kappa_2$  represents the level of residual interference at D. Note that  $\kappa_2$  shows similar behavior like  $\kappa_1$ .

### C. Sum capacity

The end-to-end rate of a multi-hop cooperative network is determined by the weakest link. So, the achievable rate related to  $s_1$  is depicted by

$$C_1 = \frac{1}{2} \log_2 (1 + \min(\gamma_{s_1 \rightarrow s_2}^1, \gamma_{s_1}^1)), \quad (6)$$

The achievable rate associated with  $s_2$  is dependent on (2) and (4), which can be denoted by

$$C_2 = \frac{1}{2} \log_2 (1 + \min(\gamma_{s_2}^1, \gamma_{s_2}^2)), \quad (7)$$

By using (5), the achievable rate related to  $s_3$  is given by

$$C_3 = \frac{1}{2} \log_2 (1 + \gamma_{s_3}^2), \quad (8)$$

Therefore, the sum capacity of the proposed DU-CNOMA system can be calculated by summing up (6), (7), and (8) as follows

$$C_{\text{sum}}^{\text{prop}} = C_1 + C_2 + C_3. \quad (9)$$

## III. CAPACITY ANALYSIS

The closed-form ESC expression of the proposed DU-CNOMA is derived over independent Rayleigh fading channel, in this section.

### A. Ergodic capacity related to $s_1$

The achievable rate of (6), can be simplified as (eq. (8))[15]

$$C_1 = \frac{1}{2} \log_2 (1 + \min\{|h_1|^2, |h_2|^2\} \rho) - \frac{1}{2} \log_2 (1 + \min\{|h_1|^2, |h_2|^2\} \rho \phi_2), \quad (10)$$

Let  $W \triangleq \min(|h_1|^2, |h_2|^2)$ . Applying PDF  $f_{|h_1|^2}(w) = (1/\lambda_1) e^{-w/\lambda_1}$  for  $i \in \{1, 2\}$ , the CDF of  $W$  is derived as  $F_W(w) = 1 - e^{-w(\frac{1}{\lambda_1} + \frac{1}{\lambda_2})}$ . Then, the probability density function of  $W$  is derived by taking the derivative of  $F_W(w)$  as

$$f_W(w) = \left( \frac{1}{\lambda_1} + \frac{1}{\lambda_2} \right) e^{-w(\frac{1}{\lambda_1} + \frac{1}{\lambda_2})} \quad (11)$$

Now, using (10) and (11), the EC associated with  $s_1$  can be obtained as

$$\begin{aligned} \bar{C}_1^{\text{ex}} &= \mathbb{E}\{C_1\} \\ &= \frac{1}{2} \int_0^\infty \{\log_2(1 + \rho w) - \log_2(1 + \rho w \phi_2)\} f_W(w) dw \end{aligned} \quad (12)$$

Using  $\log_2(x) = \frac{\ln(x)}{\ln 2}$ , (12) can be written as

$$\bar{C}_1^{\text{ex}} = \frac{1}{2 \ln 2} \int_0^\infty \{\ln(1 + \rho w) - \ln(1 + \rho w \phi_2)\} f_W(w) dw \quad (13)$$

By applying  $\int_0^\infty e^{-mw} \ln(1 + nw) dw = -\frac{1}{m} e^{m/n} \text{Ei}(-m/n)$  (eq. (4.337.2)[22]),

$$\begin{aligned} \bar{C}_1^{\text{ex}} &= -\frac{1}{2 \ln 2} e^{\frac{1}{\rho}(\frac{1}{\lambda_1} + \frac{1}{\lambda_2})} \text{Ei}\left(-\frac{1}{\rho} \left(\frac{1}{\lambda_1} + \frac{1}{\lambda_2}\right)\right) \\ &\quad + \frac{1}{2 \ln 2} e^{\frac{1}{\phi_2 \rho}(\frac{1}{\lambda_1} + \frac{1}{\lambda_2})} \text{Ei}\left(-\frac{1}{\phi_2 \rho} \left(\frac{1}{\lambda_1} + \frac{1}{\lambda_2}\right)\right) \end{aligned} \quad (14)$$

where  $\mathbb{E}\{\cdot\}$  and  $\text{Ei}\{\cdot\}$  denote the expectation operator and exponential integral function, respectively [22].

### B. Ergodic capacity related to $s_2$

Let  $U \triangleq \gamma_{s_2}^1$ ,  $V \triangleq \gamma_{s_2}^2$ , and  $Z \triangleq \min(U, V)$ . The CDF of  $U$  and  $V$  can be respectively written as

$$\begin{aligned} F_U(u) &= 1 - \frac{\phi_2 \lambda_2}{\phi_2 \lambda_2 + \phi_1 \kappa_1 \lambda_2 v} e^{-\frac{u}{\phi_2 \rho \lambda_2}} \\ &= 1 - \frac{p}{p + u} e^{-\frac{u}{\phi_2 \rho \lambda_2}}, \end{aligned} \quad (15)$$

$$\begin{aligned} F_V(v) &= 1 - \frac{\vartheta_2 \lambda_3}{\vartheta_2 \lambda_3 + \vartheta_3 \lambda_1 v} e^{-\frac{v}{\vartheta_2 \rho \lambda_3}} \\ &= 1 - \frac{g}{g + v} e^{-\frac{v}{\vartheta_2 \rho \lambda_3}}, \end{aligned} \quad (16)$$

where  $p = \phi_2 \lambda_2 / \phi_1 \kappa_1 \lambda_2$  and  $g = \vartheta_2 \lambda_3 / \vartheta_3 \lambda_1$ . Using (15) and (16), the CDF of  $Z$  can be obtained as

$$F_Z(z) = 1 - \frac{pg}{(p+z)(g+z)} e^{-qz}, \quad (17)$$

where  $q = \frac{1}{\phi_2 \rho \lambda_2} + \frac{1}{\vartheta_2 \rho \lambda_3}$ . So, the exact EC related to  $s_2$  is derived as

$$\bar{C}_2^{\text{ex}} = \mathbb{E}\{C_2\} = \frac{1}{2} \int_0^\infty \log_2(1+z) f_Z(z) dz. \quad (18)$$

Applying  $\int_0^\infty \log_2(1+z) f_Z(z) dz = \frac{1}{\ln 2} \int_0^\infty \frac{1-F_Z(z)}{1+z} dz$ , (18) can be represented as

$$\begin{aligned} \bar{C}_2^{\text{ex}} &= \frac{1}{2 \ln 2} \int_0^\infty \frac{pg}{(1+z)(p+z)(g+z)} e^{-qz} dz \\ &= \frac{p \log_2 e}{2(p-1)} \int_0^\infty \left[ (1+z)^{-1} \frac{g}{g+z} - (p+z)^{-1} \frac{g}{g+z} \right] e^{-qz} dz \\ &= \frac{p \log_2 e}{2(p-1)} \left[ \frac{g}{g-1} \left\{ -e^{-q} \text{Ei}(-q) + e^{gq} \text{Ei}(-gq) \right\} \right. \\ &\quad \left. - \frac{g}{g-p} \left\{ -e^{pq} \text{Ei}(-pq) + e^{gq} \text{Ei}(-gq) \right\} \right]. \end{aligned} \quad (19)$$

Note that (19) is derived by considering imperfect SIC (i.e.,  $0 < \kappa_1 \leq 1$ ). Therefore, the exact EC of  $s_2$  under perfect SIC is derived as follows.

With perfect SIC,  $Z \triangleq \min(U, V)$  can be written as  $Z \triangleq \min(\phi_2 \rho |h_2|^2, V)$ . The CDF of  $Z$  is therefore given by

$$F_Z(z) = 1 - \frac{g}{g+z} e^{-qz}, \quad (20)$$

The exact EC related to  $s_2$  under perfect SIC, is derived as

$$\begin{aligned} \bar{C}_{2,p}^{\text{ex}} &= \frac{1}{2} \int_0^\infty \log_2(1+z) f_Z(z) dz \\ &= \frac{\log_2 e}{2} \int_0^\infty \frac{g}{(1+z)(g+z)} e^{-qz} dz \\ &= \frac{g \log_2 e}{2(g-1)} \int_0^\infty \left( \frac{1}{1+z} - \frac{1}{g+z} \right) e^{-qz} dz \\ &= \frac{g \log_2 e}{2(g-1)} \{-e^{-q} \text{Ei}(-q) + e^{gq} \text{Ei}(-gq)\}. \end{aligned} \quad (21)$$

### C. Ergodic capacity related to $s_3$

Let  $Y \triangleq \gamma_{s_3}^2$ . So, the CDF of  $Y$  is derived as

$$F_Y(y) = 1 - \frac{\vartheta_3 \lambda_1}{\vartheta_3 \lambda_1 + \vartheta_2 \kappa_2 \lambda_3 y} e^{-\frac{y}{\vartheta_3 \rho \lambda_1}}. \quad (22)$$

So, the exact EC associated with  $s_3$  is obtained as

$$\begin{aligned} \bar{C}_3^{\text{ex}} &= \mathbb{E}\{C_3\} = \frac{1}{2} \int_0^\infty \log_2(1+y) f_Y(y) dy \\ &= \frac{\log_2 e}{2} \int_0^\infty (1+y)^{-1} \frac{\vartheta_3 \lambda_1}{\vartheta_3 \lambda_1 + \vartheta_2 \kappa_2 \lambda_3 y} e^{-\frac{y}{\vartheta_3 \rho \lambda_1}} dy \\ &= \frac{\log_2 e}{2} \left[ \frac{\vartheta_3 \lambda_1}{\vartheta_3 \lambda_1 - \vartheta_2 \kappa_2 \lambda_3} \right. \\ &\quad \left. \times \left\{ \int_0^\infty (1+y)^{-1} - \int_0^\infty \frac{\vartheta_2 \kappa_2 \lambda_3}{\vartheta_3 \lambda_1 + \vartheta_2 \kappa_2 \lambda_3 y} \right\} e^{-\frac{y}{\vartheta_3 \rho \lambda_1}} dy \right] \\ &= \frac{\log_2 e}{2} \left[ \frac{\vartheta_3 \lambda_1}{\vartheta_3 \lambda_1 - \vartheta_2 \kappa_2 \lambda_3} \times \right. \\ &\quad \left. \left\{ -e^{-\frac{1}{\vartheta_3 \rho \lambda_1}} \text{Ei}\left(-\frac{1}{\vartheta_3 \rho \lambda_1}\right) + e^{\frac{1}{\vartheta_2 \kappa_2 \rho \lambda_3}} \text{Ei}\left(-\frac{1}{\vartheta_2 \kappa_2 \rho \lambda_3}\right) \right\} \right]. \end{aligned} \quad (23)$$

Note that (23) is derived by considering imperfect SIC (i.e.,  $0 < \kappa_2 \leq 1$ ). The exact EC of  $s_3$  under perfect SIC is derived as follows.

With perfect SIC,  $Y \triangleq \gamma_{s_3}^2$  can be written as  $Y \triangleq \vartheta_3 \rho |h_1|^2$ . The CDF of  $Y$  is therefore given by

$$F_Y(y) = 1 - e^{-\frac{y}{\vartheta_3 \rho \lambda_1}}. \quad (24)$$

Hence, the exact EC associated with  $s_3$  is obtained as

$$\bar{C}_{3,p}^{\text{ex}} = \frac{\log_2 e}{2} \int_0^\infty \frac{1 - F_Y(y)}{(1+y)} dy = -\frac{\log_2 e}{2} e^r \text{Ei}(-r), \quad (25)$$

where  $r = \frac{1}{\vartheta_3 \rho \lambda_1}$ .

#### D. Ergodic sum capacity of DU-CNOMA

Using (14), (19), and (23), the exact closed-form expression of ESC of the proposed DU-CNOMA protocol under imperfect SIC can be written by

$$\bar{C}_{\text{sum, ip}}^{\text{prop}} = \bar{C}_1^{\text{ex}} + \bar{C}_2^{\text{ex}} + \bar{C}_3^{\text{ex}}. \quad (26)$$

Conversely, using (14), (21), and (25), the exact closed-form expression of ESC of the proposed DU-CNOMA protocol under perfect SIC can be written by

$$\bar{C}_{\text{sum, p}}^{\text{prop}} = \bar{C}_1^{\text{ex}} + \bar{C}_{2,p}^{\text{ex}} + \bar{C}_{3,p}^{\text{ex}}. \quad (27)$$

### IV. OUTAGE PROBABILITY ANALYSIS

According to the required quality of service,  $C_{t_1}$ ,  $C_{t_2}$ , and  $C_{t_3}$  are assumed to be the predetermined target data rate thresholds of the symbols  $s_1$ ,  $s_2$ , and  $s_3$ , respectively. The closed-form expressions of outage probabilities related to  $s_1$ ,  $s_2$ , and  $s_3$  are provided over independent Rayleigh fading channel in the following subsections.

#### A. Outage probability of symbol $s_1$

The OP of symbol  $s_1$  is given by

$$\begin{aligned} P_{\text{out},s_1} &= P_r\{\gamma_{s_1}^1 < R_{t_1}\} \\ &= 1 - e^{-\frac{R_{t_1}}{\lambda_1 \rho (\phi_1 - \phi_2 R_{t_1})}}, \end{aligned} \quad (28)$$

where  $R_{t_1} = 2^{2C_{t_1}} - 1$  and  $\frac{R_{t_1}}{R_{t_1} + 1} < \phi_1 < 1$ .

#### B. Outage probability of symbol $s_2$

The OP of symbol  $s_2$  is given by

$$\begin{aligned} P_{\text{out},s_2} &= 1 - P_r\{\min(\gamma_{s_2}^1, \gamma_{s_2}^2) > R_{t_2}\} P_r\{\gamma_{s_1 \rightarrow s_2}^1 > R_{t_1}\} \\ &= 1 - \frac{\vartheta_2 \lambda_2 \vartheta_2 \lambda_3}{(\vartheta_2 \lambda_2 + \phi_1 \kappa_1 \lambda_2 R_{t_2})(\vartheta_2 \lambda_3 + \vartheta_3 \lambda_1 R_{t_2})} \\ &\quad \times e^{-\frac{R_{t_2}}{\vartheta_2 \rho \lambda_2} - \frac{R_{t_2}}{\vartheta_2 \rho \lambda_3} - \frac{R_{t_1}}{\lambda_2 \rho (\phi_1 - \phi_2 R_{t_1})}}, \end{aligned} \quad (29)$$

where  $R_{t_2} = 2^{2C_{t_2}} - 1$ . Now, by putting  $\kappa_1=0$ , the OP of  $s_2$  under perfect SIC can be expressed as

$$P_{\text{out},s_2}^{\text{p}} = 1 - \frac{\vartheta_2 \lambda_3}{(\vartheta_2 \lambda_3 + \vartheta_3 \lambda_1 R_{t_2})} e^{-\frac{R_{t_2}}{\vartheta_2 \rho \lambda_2} - \frac{R_{t_2}}{\vartheta_2 \rho \lambda_3} - \frac{R_{t_1}}{\lambda_2 \rho (\phi_1 - \phi_2 R_{t_1})}} \quad (30)$$

#### C. Outage probability of symbol $s_3$

The OP of symbol  $s_3$  is given by

$$P_{\text{out},s_3} = 1 - \frac{\vartheta_3 \lambda_1}{\vartheta_3 \lambda_1 + \vartheta_2 \kappa_2 \lambda_3 R_{t_3}} e^{-\frac{R_{t_3}}{\vartheta_3 \rho \lambda_1}}, \quad (31)$$

where  $R_{t_3} = 2^{2C_{t_3}} - 1$ . Now, by putting  $\kappa_2=0$ , the OP of  $s_3$  under perfect SIC can be expressed as

$$P_{\text{out},s_3}^{\text{p}} = 1 - e^{-\frac{R_{t_3}}{\vartheta_3 \rho \lambda_1}}. \quad (32)$$

### V. OUTAGE CAPACITY ANALYSIS

This section presents analytical derivation for OSC of the proposed DU-CNOMA over independent Rayleigh fading channel.

#### A. Outage capacity of $s_1$

The OC  $C_{t_1}$  related to  $s_1$ , with specified OP  $\Upsilon_1$  can be computed from (28) as

$$\begin{aligned} \Upsilon_1 &= 1 - e^{-\frac{R_{t_1}}{\lambda_1 \rho (\phi_1 - \phi_2 R_{t_1})}} \\ e^{-\frac{R_{t_1}}{\lambda_1 \rho (\phi_1 - \phi_2 R_{t_1})}} &= 1 - \Upsilon_1 \\ -\frac{R_{t_1}}{\lambda_1 \rho (\phi_1 - \phi_2 R_{t_1})} &= \ln(1 - \Upsilon_1) \\ \{(\lambda_1 \phi_2 \rho \ln(1 - \Upsilon_1) - 1)R_{t_1} &= \lambda_1 \phi_1 \rho \ln(1 - \Upsilon_1) \\ 2^{2C_{t_1}} - 1 &= \frac{\lambda_1 \phi_1 \rho \ln(1 - \Upsilon_1)}{(\lambda_1 \phi_2 \rho \ln(1 - \Upsilon_1) - 1)} \\ C_{t_1} &= \frac{1}{2} \log_2 \left( 1 + \frac{\lambda_1 \phi_1 \rho \ln(1 - \Upsilon_1)}{(\lambda_1 \phi_2 \rho \ln(1 - \Upsilon_1) - 1)} \right). \end{aligned} \quad (33)$$

#### B. Outage capacity of $s_2$

Using  $e^x \approx 1 + x$  at high  $\rho$ , the OC  $C_{t_2}$  related to  $s_2$ , with specified OP  $\Upsilon_2$  can be computed from (29) as

$$\begin{aligned} \Upsilon_2 &= 1 - \frac{\vartheta_2 \lambda_2 \vartheta_2 \lambda_3}{(\vartheta_2 \lambda_2 + \phi_1 \kappa_1 \lambda_2 R_{t_2})(\vartheta_2 \lambda_3 + \vartheta_3 \lambda_1 R_{t_2})} \\ &\quad \times \left( 1 - \frac{R_{t_2}}{\vartheta_2 \rho \lambda_2} - \frac{R_{t_2}}{\vartheta_2 \rho \lambda_3} \right) \\ \Upsilon_2 &= 1 - \frac{GH}{(G + IR_{t_2})(H + JR_{t_2})} \left( 1 - \frac{R_{t_2}}{G\rho} - \frac{R_{t_2}}{H\rho} \right), \end{aligned} \quad (34)$$

conditioned on  $\gamma_{s_1 \rightarrow s_2}^1 > R_{t_1}$ , where  $G = \vartheta_2 \lambda_2$ ,  $H = \vartheta_2 \lambda_3$ ,  $I = \phi_1 \kappa_1 \lambda_2$ , and  $J = \vartheta_3 \lambda_1$ . After some algebraic simplifications, (34) can be rewritten as

$$\begin{aligned} IJ\rho(1 - \Upsilon_2)R_{t_2}^2 + \{(GJ + HI)(1 - \Upsilon_2)\rho + H + G\}R_{t_2} + (-GH\rho\Upsilon_2) &= 0 \\ KR_{t_2}^2 + LR_{t_2} + M &= 0 \end{aligned} \quad (35)$$

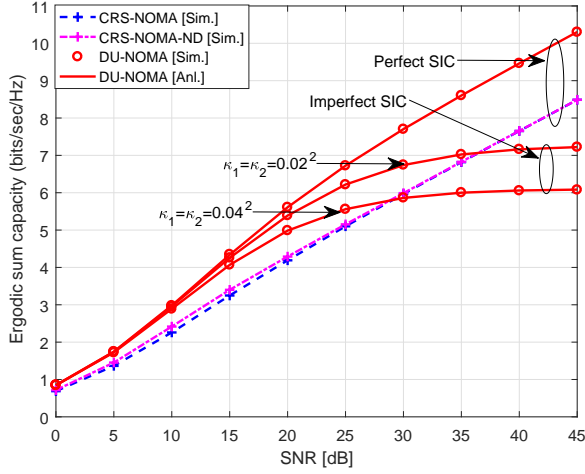


Fig. 2. ESC comparison between CRS-NOMA [15], CRS-NOMA-ND [17], and proposed DU-CNOMA w.r.t SNR  $\rho$ .  $\phi_1=0.9$ ,  $\phi_2=0.1$ ,  $\vartheta_2=1$ , and  $\vartheta_3=0.3$ .

where  $K = IJ\rho(1 - \Upsilon_2)$ ,  $L = (GJ + HI)(1 - \Upsilon_2)\rho + H + G$ ,  $M = -GH\rho\Upsilon_2$  are assumed. Solving (35) and considering feasible root,  $C_{t_2}$  can be obtained as

$$\begin{aligned} R_{t_2} &= \frac{-L + \sqrt{L^2 - 4KM}}{2K} \\ 2^{2C_{t_2}} - 1 &= \frac{-L + \sqrt{L^2 - 4KM}}{2K} \\ C_{t_2} &= \frac{1}{2} \log_2 \left( 1 + \frac{-L + \sqrt{L^2 - 4KM}}{2K} \right) \end{aligned} \quad (36)$$

On the other hand, the OC  $C_{t_2}$  under perfect SIC can be computed from (30) as

$$\begin{aligned} \Upsilon_2 &= 1 - \frac{\vartheta_2 \lambda_3}{(\vartheta_2 \lambda_3 + \vartheta_3 \lambda_1 R_{t_2})} \left( 1 - \frac{R_{t_2}}{\vartheta_2 \rho \lambda_2} - \frac{R_{t_2}}{\vartheta_2 \rho \lambda_3} \right) \\ &= 1 - \frac{H}{(H + JR_{t_2})} \left( 1 - \frac{R_{t_2}}{G\rho} - \frac{R_{t_2}}{H\rho} \right) \\ R_{t_2} &= \frac{GH\rho\Upsilon_2}{GJ\rho(1 - \Upsilon_2) + G + H} \\ C_{t_2} &= \frac{1}{2} \log_2 \left( 1 + \frac{GH\rho\Upsilon_2}{GJ\rho(1 - \Upsilon_2) + G + H} \right) \end{aligned} \quad (37)$$

### C. Outage capacity of $s_3$

Using  $e^x \approx 1 + x$  at high  $\rho$ , the OC  $C_{t_3}$  related to  $s_3$ , with specified OP  $\Upsilon_3$  can be computed from (31) as

$$\begin{aligned} \Upsilon_3 &= 1 - \frac{\vartheta_3 \lambda_1}{\vartheta_3 \lambda_1 + \vartheta_2 \kappa_2 \lambda_3 R_{t_3}} \left( 1 - \frac{R_{t_3}}{\vartheta_3 \rho \lambda_1} \right) \\ \Upsilon_3 &= 1 - \frac{\vartheta_3 \lambda_1 (\vartheta_3 \rho \lambda_1 - R_{t_3})}{(\vartheta_3 \lambda_1 + \vartheta_2 \kappa_2 \lambda_3 R_{t_3}) \vartheta_3 \rho \lambda_1} \\ \Upsilon_3 &= \frac{\vartheta_2 \kappa_2 \lambda_3 R_{t_3} \rho + R_{t_3}}{(\vartheta_3 \lambda_1 + \vartheta_2 \kappa_2 \lambda_3 R_{t_3}) \rho} \\ R_{t_3} &= \frac{\vartheta_3 \lambda_1 \rho \Upsilon_3}{1 + \vartheta_2 \kappa_2 \lambda_3 \rho - \vartheta_2 \kappa_2 \lambda_3 \rho \Upsilon_3} \\ C_{t_3} &= \frac{1}{2} \log_2 \left( 1 + \frac{\vartheta_3 \lambda_1 \rho \Upsilon_3}{1 + \vartheta_2 \kappa_2 \lambda_3 \rho (1 - \Upsilon_3)} \right) \end{aligned} \quad (38)$$

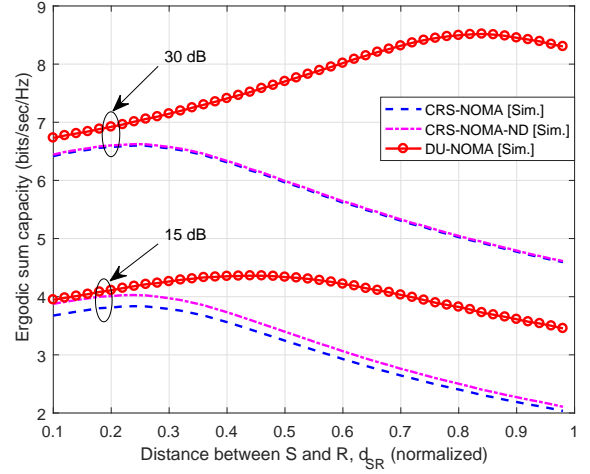


Fig. 3. ESC comparison between CRS-NOMA [15], CRS-NOMA-ND [17], and proposed DU-CNOMA w.r.t normalized distance from S to R,  $d_{SR}$  under perfect SIC.  $\phi_1=0.9$ ,  $\phi_2=0.1$ ,  $\vartheta_2=1$ , and  $\vartheta_3=0.3$ .

On the other hand, the OC  $C_{t_3}$  under perfect SIC can be computed from (32) as

$$\begin{aligned} \Upsilon_3 &= 1 - e^{-\frac{R_{t_3}}{\vartheta_3 \rho \lambda_1}} \\ e^{-\frac{R_{t_3}}{\vartheta_3 \rho \lambda_1}} &= 1 - \Upsilon_3 \\ R_{t_3} &= -\vartheta_3 \rho \lambda_1 \ln(1 - \Upsilon_3) \\ 2^{2C_{t_3}} &= 1 - \vartheta_3 \rho \lambda_1 \ln(1 - \Upsilon_3) \\ C_{t_3} &= \frac{1}{2} \log_2 (1 - \vartheta_3 \rho \lambda_1 \ln(1 - \Upsilon_3)) \end{aligned} \quad (39)$$

### D. Outage sum capacity

Using (33), (36), and (38), the OSC of the proposed DU-CNOMA under imperfect SIC is given by

$$C_{\text{sum, ip}}^{\text{out}} = (33) + (36) + (38). \quad (40)$$

Conversely, Using (33), (37), and (39), the OSC of the proposed DU-CNOMA under perfect SIC is given by

$$C_{\text{sum, p}}^{\text{out}} = (33) + (37) + (39). \quad (41)$$

## VI. NUMERICAL RESULTS

This section presents simulation (Sim.) and analytical (Anl.) results of our proposed DU-CNOMA protocol. In each case, analytical result matches well with simulation result and it confirms the correctness of the author's analysis presented here. For comparison purpose, the simulation results for CRS-NOMA [15] and CRS-NOMA-ND [17] are also presented. It should be mentioned that analytical derivations for OP and OSC are not provided in [15, 17]. Throughout the simulation, it is assumed that  $v=3$ ,  $d_{SD}=1$ ,  $d_{SR} = d_{SD}/2$ ,  $d_{RD} = 1 - d_{SR}$ ,  $\phi_1=0.9$ ,  $\phi_2=0.1$ ,  $\Upsilon_1 = \Upsilon_2 = \Upsilon_3 = \Upsilon$ ,  $\vartheta_2=1$ , and  $\vartheta_3=0.3$ , unless otherwise specified. Note that fixed power allocation method as in [15-17] is assumed for the proposed protocol.

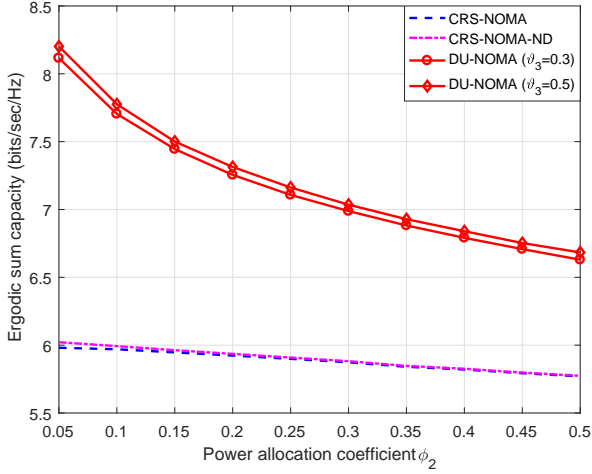


Fig. 4. ESC comparison between CRS-NOMA [15], CRS-NOMA-ND [17], and proposed DU-CNOMA w.r.t power allocation coefficient  $\phi_2$  under perfect SIC.  $\vartheta_2=1$ .

#### A. Ergodic capacity

ESC versus SNR behavior of DU-CNOMA, CRS-NOMA, and CRS-NOMA-ND is shown in Fig. 2. Performance of the proposed DU-CNOMA is executed under two conditions, i.e., perfect SIC and imperfect SIC. Note that only perfect SIC is considered in CRS-NOMA and CRS-NOMA-ND. For the case of perfect SIC, it is observed from the figure that DU-CNOMA significantly outperforms all other existing protocols. However, with the increasing amount of residual interference the performance of DU-CNOMA starts degrading which causes it to exhibit a saturated value at medium to high  $\rho$  values. The performance of the proposed protocol becomes worse for  $\kappa_1 = \kappa_2 = 0.04^2$  than  $\kappa_1 = \kappa_2 = 0.02^2$ . Therefore, at high  $\rho$ , the adverse impact of residual interference on DU-CNOMA causes it to achieve less ESC than existing methods. Therefore, it is suggested that an efficient interference cancellation technique can significantly improve the performance of DU-NOMA, particularly at medium to high  $\rho$ . Lastly, strong agreement between simulation and analytical results verifies the appropriateness of the ESC analysis.

ESC behavior for varying relay position between source and destination,  $d_{SR}$  is demonstrated in Fig. 3, under perfect SIC. ESC versus  $d_{SR}$  performance of DU-CNOMA is compared with CRS-NOMA and CRS-NOMA-ND protocols for two different  $\rho$  values, i.e.,  $\rho = 15$  and 30 dB. For both cases, proposed protocol achieves better ESC than existing protocols irrespective of the relay position. In addition, ESC of DU-CNOMA becomes far better than others for the increasing distance between source and relay. However, this behavior is bounded by a maximum  $d_{SR}$  value (e.g., around  $d_{SR} = 0.5$  for  $\rho = 15$  dB and around  $d_{SR} = 0.8$  for  $\rho = 30$  dB).

ESC with respect to (w.r.t) the power allocation coefficient  $\phi_2$  is shown in Fig. 4, where  $\vartheta_2 = 1$  and  $\vartheta_3 = 0.3$  or 0.5. It is demonstrated that the ESC performance of all protocols degrades with the increase of  $\phi_2$ . Further, ESC of the proposed DU-CNOMA protocol is higher than existing protocols for all feasible values of  $\phi_2$ . It is also clear from the figure that ESC

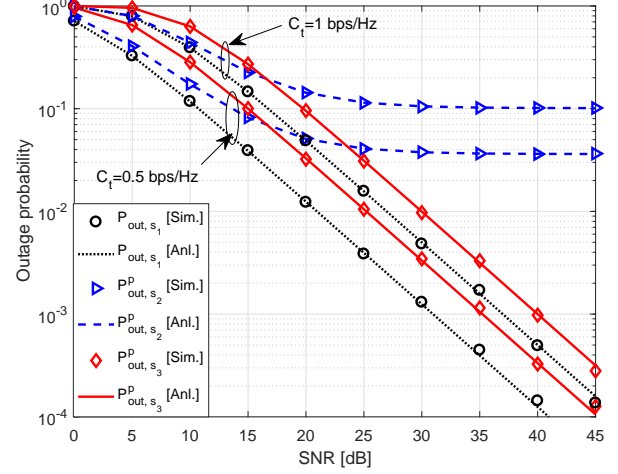


Fig. 5. OP of the proposed DU-CNOMA w.r.t SNR  $\rho$  under perfect SIC.  $\phi_1=0.9$ ,  $\phi_2=0.1$ ,  $\vartheta_2=1$ , and  $\vartheta_3=0.3$ .

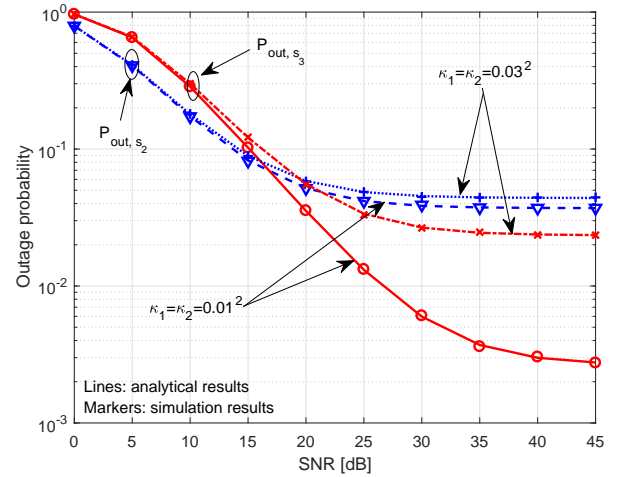


Fig. 6. OP of the proposed DU-CNOMA w.r.t SNR  $\rho$  under imperfect SIC.  $\phi_1=0.9$ ,  $\phi_2=0.1$ ,  $\vartheta_2=1$ ,  $\vartheta_3=0.3$ , and  $C_t=0.5$  bps/Hz.

of the proposed protocol is higher for  $\vartheta_3 = 0.5$  than 0.3.

#### B. Outage probability

OP versus SNR performance of the proposed protocol is demonstrated in Fig. 5 for two different threshold values of target data rate, i.e.,  $C_t = 1$  and 0.5 (bps/Hz)s. Perfect SIC is considered for analyzing all analytical and simulation results. Coincidence of analytical and simulation results for each case refers to the accuracy of OP analysis. OP becomes better with the increase of SNR wherein OP related to symbol  $s_1$  is less than  $s_2$  and  $s_3$  for a specific  $C_t$  value. Though OPs related to symbols  $s_1$  and  $s_3$  decrease linearly with the increase of  $\rho$ , OP related to symbol  $s_2$  takes a saturated value for medium to high  $\rho$  range. The reason behind exhibiting this performance by  $s_2$  is the interference effect from other symbols on it. The OP related to  $s_1$ ,  $s_2$ , and  $s_3$  for  $C_t = 1$  bps/Hz is higher than  $C_t = 0.5$  bps/Hz, as expected.



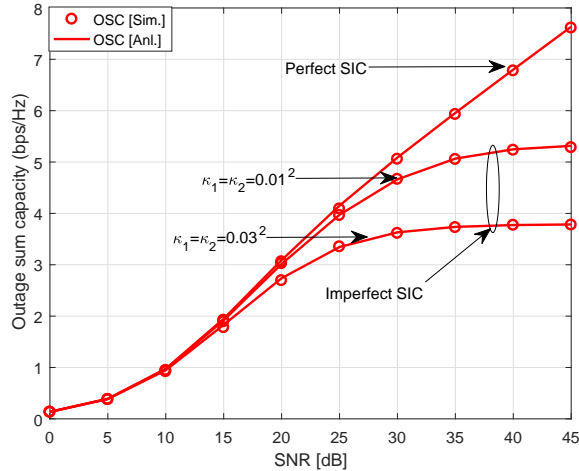


Fig. 7. OSC of the proposed DU-CNOMA w.r.t SNR  $\rho$ .  $\phi_1=0.9$ ,  $\phi_2=0.1$ ,  $\vartheta_2=1$ ,  $\vartheta_3=0.3$ , and  $\Upsilon=0.1$ .

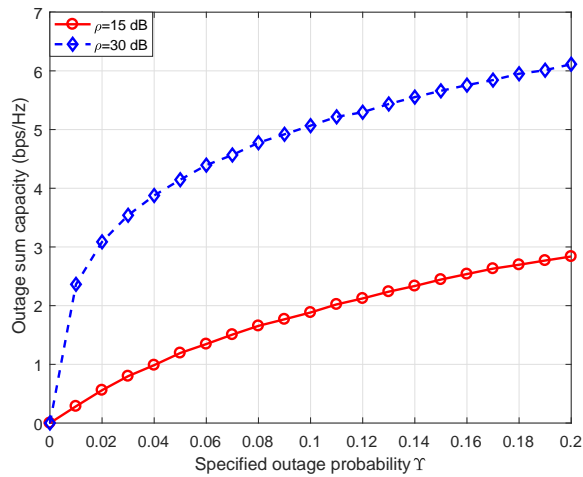


Fig. 8. OSC of the proposed DU-CNOMA w.r.t specified outage probability  $\Upsilon$  under perfect SIC.  $\phi_1=0.9$ ,  $\phi_2=0.1$ ,  $\vartheta_2=1$ , and  $\vartheta_3=0.3$ .

By considering imperfect SIC and target data rate  $C_1 = 0.5$  bps/Hz, OP of DU-CNOMA protocol w.r.t SNR  $\rho$  is depicted in Fig. 6. Only OP versus SNR analysis related to  $s_2$  and  $s_3$  are compared as the performance related to  $s_1$  is not affected by imperfect SIC condition. OP related to  $s_2$  is better than  $s_3$  at low to medium  $\rho$  ( $0 < \rho \leq 15$ ), whereas OP related to  $s_3$  becomes better than  $s_2$  at high  $\rho$  ( $\rho > 15$ ) for the considered parameters. OP related to any of the symbols is less for small residual interference (i.e.,  $\kappa_1 = \kappa_2 = 0.01^2$ ) than comparatively large amount of residual interference (i.e.,  $\kappa_1 = \kappa_2 = 0.03^2$ ). Though OP related to  $s_3$  shows linear behavior even at high  $\rho$  as shown in Fig. 5, it tends to be saturated at high  $\rho$  as shown in Fig. 6 due to the impact of residual interference.

### C. Outage capacity

10% OSC of the proposed DU-CNOMA protocol w.r.t SNR  $\rho$  is plotted under both perfect and imperfect SIC conditions in Fig. 7. Two cases of imperfect SIC is considered, i.e.,  $\kappa_1 = \kappa_2$

$= 0.01^2$  and  $\kappa_1 = \kappa_2 = 0.03^2$ . For perfect SIC condition, OSC of the system linearly increases with the betterment of  $\rho$  and maintains it till the high  $\rho$ . But, For imperfect SIC condition, OSC of the system only increases linearly upto medium value of  $\rho$ , then it becomes saturated due to the impact of residual interference. If the effect of residual interference increases, OSC of DU-CNOMA decreases and tends to be saturated at a less value of  $\rho$  than for comparatively small residual interference impact.

OSC behavior w.r.t specified outage probability  $\Upsilon$  for the proposed DU-CNOMA protocol is demonstrated in Fig. 8. Perfect SIC condition is taken into account and the performance behavior is observed for two different values of  $\rho$ , i.e.,  $\rho = 15$  dB and 30 dB. Fig. 8 depicts that OSC of the system increases with the increase of specified outage probability  $\Upsilon$ . In addition, OSC goes high for higher  $\rho$  ( $\rho = 30$  dB) than lower  $\rho$  ( $\rho = 15$  dB).

## VII. CONCLUSION AND FUTURE WORKS

A cooperative decode-and-forward relaying strategy using the concept of downlink and uplink NOMA has proposed and analyzed in this paper. Under both perfect and imperfect SIC, the performance of the proposed protocol has studied comprehensively, in terms of ESC, OP, and OSC over independent Rayleigh fading channels. The closed-form expressions of these system parameters have derived and validated by computer simulation. It has shown that the proposed protocol significantly outperforms CRS-NOMA and CRS-NOMA-ND under perfect SIC, whereas under imperfect SIC, performance gains depends on the level of residual interference, particularly at high SNR. Furthermore, hybrid downlink-uplink NOMA for multi-input multi-output systems will be investigated in future works.

## DISCLOSURE STATEMENT

The author(s) declare(s) no potential conflict of interest regarding the publication of this paper.

## REFERENCES

- [1] S. Chen and J. Zhao, "The requirements, challenges, and technologies for 5G of terrestrial mobile telecommunication," *IEEE Commun. Mag.*, vol. 52, no. 5, pp. 36–43, May 2014.
- [2] W. H. Chin, Z. Fan, and R. Haines, "Emerging technologies and research challenges for 5G wireless networks," *IEEE Wireless Commun.*, vol. 21, no. 2, pp. 106–112, Apr. 2014.
- [3] J. N. Laneman, D. N. C. Tse, and G. W. Wornell, "Cooperative diversity in wireless networks: Efficient protocols and outage behavior," *IEEE Trans. Inf. Theory*, vol. 50, no. 12, pp. 3062–3080, Dec. 2004.
- [4] V. W. Wong, R. Schober, D. W. K. Ng, and L.-C. Wang, *Key Technologies for 5G Wireless Systems*. Cambridge university press, 2017.
- [5] S. M. R. Islam, N. Avazov, O. A. Dobre, and K. S. Kwak, "Power-domain non-orthogonal multiple access (NOMA) in 5G systems: Potentials and challenges," *IEEE Commun. Surveys Tuts.*, vol. 19, no. 2, pp. 721–742, Secondquarter 2017.
- [6] L. Dai, B. Wang, Y. Yuan, S. Han, C. I. I, and Z. Wang, "Non-orthogonal multiple access for 5G: Solutions, challenges, opportunities, and future research trends," *IEEE Commun. Mag.*, vol. 53, no. 9, pp. 74–81, Sept. 2015.
- [7] Z. Ding, M. Peng, and H. V. Poor, "Cooperative non-orthogonal multiple access in 5G systems," *IEEE Commun. Lett.*, vol. 19, no. 8, pp. 1462–1465, Aug. 2015.

- [8] M. F. Kader, M. B. Shahab, and S. Y. Shin, "Non-orthogonal multiple access for a full-duplex cooperative network with virtually paired users," *Computer Commun.*, vol. 120, pp. 1 – 9, 2018.
- [9] D. Wan, M. Wen, F. Ji, H. Yu, and F. Chen, "Non-orthogonal multiple access for cooperative communications: Challenges, opportunities, and trends," *IEEE Wireless Commun.*, vol. 25, no. 2, pp. 109–117, April 2018.
- [10] Z. Ding, X. Lei, G. K. Karagiannidis, R. Schober, J. Yuan, and V. K. Bhargava, "A survey on non-orthogonal multiple access for 5G networks: Research challenges and future trends," *IEEE J. Sel. Areas Commun.*, vol. 35, no. 10, pp. 2181–2195, Oct. 2017.
- [11] M. F. Kader and S. Y. Shin, "Cooperative relaying using space-time block coded non-orthogonal multiple access," *IEEE Trans. Veh. Technol.*, vol. 66, no. 7, pp. 5894–5903, Jul. 2017.
- [12] X. Liang, Y. Wu, D. W. K. Ng, Y. Zuo, S. Jin, and H. Zhu, "Outage performance for cooperative NOMA transmission with an AF relay," *IEEE Commun. Lett.*, vol. 21, no. 11, pp. 2428–2431, Nov. 2017.
- [13] M. F. Kader and S. Y. Shin, "Coordinated direct and relay transmission using uplink NOMA," *IEEE Wireless Commun. Lett.*, vol. 7, no. 3, pp. 1–4, Jun. 2017.
- [14] W. Shin, H. Yang, M. Vaezi, J. Lee, and H. V. Poor, "Relay-aided NOMA in uplink cellular networks," *IEEE Signal Process. Lett.*, vol. 24, no. 12, pp. 1842–1846, Dec. 2017.
- [15] J. B. Kim and I. H. Lee, "Capacity analysis of cooperative relaying systems using non-orthogonal multiple access," *IEEE Commun. Lett.*, vol. 19, no. 11, pp. 1949–1952, Nov. 2015.
- [16] R. Jiao, L. Dai, J. Zhang, R. MacKenzie, and M. Hao, "On the performance of NOMA-based cooperative relaying systems over Rician fading channels," *IEEE Transactions on Vehicular Technology*, vol. 66, no. 12, pp. 11 409–11 413, Dec. 2017.
- [17] M. Xu, F. Ji, M. Wen, and W. Duan, "Novel receiver design for the cooperative relaying system with non-orthogonal multiple access," *IEEE Commun. Lett.*, vol. 20, no. 8, pp. 1679–1682, Aug. 2016.
- [18] M. S. Ali, H. Tabassum, and E. Hossain, "Dynamic user clustering and power allocation for uplink and downlink non-orthogonal multiple access (NOMA) systems," *IEEE Access*, vol. 4, pp. 6325–6343, 2016.
- [19] Z. Yang, Z. Ding, P. Fan, and N. Al-Dhahir, "A general power allocation scheme to guarantee quality of service in downlink and uplink NOMA systems," *IEEE Trans. Wireless Commun.*, vol. 15, no. 11, pp. 7244–7257, Nov. 2016.
- [20] M. F. Kader, M. B. Shahab, and S. Y. Shin, "Exploiting non-orthogonal multiple access in cooperative relay sharing," *IEEE Commun. Lett.*, vol. 21, no. 5, pp. 1159–1162, May 2017.
- [21] Z. Wei, L. Dai, D. W. K. Ng, and J. Yuan, "Performance analysis of a hybrid downlink-uplink cooperative noma scheme," in *2017 IEEE 85th Vehicular Technology Conference (VTC Spring)*, Jun. 2017, pp. 1–7.
- [22] I. S. Gradshteyn and I. M. Ryzhik, *Table of integrals, series and products 7th edn.* New York, NY, USA: Academic, 2007.